

## Extended electronic states above metal-doped carbon nanostructures

Stanislav R. Stoyanov, Petr Král,<sup>a)</sup> and Boyang Wang

Department of Chemistry, University of Illinois at Chicago, Chicago, Illinois 60607

(Received 18 December 2006; accepted 24 February 2007; published online 11 April 2007)

Spatially extended electronic states formed above metal atoms covalently attached to carbon nanostructures are presented by *ab initio* calculations. These extended states are largely composed of the unpopulated 5–6s atomic orbitals of the metal atom. They could be manipulated by electric and optical fields and used in electron emission. The metallic sites can also facilitate binding and releasing of ions, atoms, and molecular ligands, so the structures can serve as “atomic nanotools.”

© 2007 American Institute of Physics. [DOI: 10.1063/1.2721131]

Spatially extended Rydberg states that form in atoms and molecules can have numerous applications.<sup>1,2</sup> We have suggested that extended states could also form above metallic carbon nanotubes (CNTs),<sup>3,4</sup> when electrons spin around their mirror images in the CNTs. Recently, these “tubular image states” with long lifetimes were observed in photoexcitation experiments.<sup>5</sup> In general, the presence of extended electronic states above nanosystems might allow the design of unique electron emission, absorption, and storage devices. These states might also facilitate temporary storage and chemical activation sites for atoms and molecules that are later deposited elsewhere.

In this work, we follow this idea and investigate the *formation* and *control* of extended electronic states above metal-doped carbon nanostructures. These states could be formed in the presence of metals that have rich binding possibilities, energetically accessible unoccupied states, and a plenty of free electrons from the C structures. The metallic binding site is designed in analogy to metalloporphyrins, where a central metal atom is coordinated to four pyrrole rings.<sup>6</sup> Functionally versatile porphyrins can activate biochemical reactions<sup>7</sup> and could be used as matrices for hydrogen storage,<sup>8</sup> nanoscale materials,<sup>9</sup> and optical devices.<sup>10,11</sup>

In Fig. 1 (up), we present the studied Ni-doped tip and wall of a (4,4) single-wall carbon nanotube (SWCNT). In the left structure, Ni is attached to the four pyrrole rings,<sup>6</sup> as in metalloporphyrins,<sup>7</sup> but the four connecting methine linkers are removed. In the right structure, two C atoms are replaced with the Ni atom and the four adjacent C atoms are substituted with four N atoms.<sup>12</sup> Both complexes are ended with H atoms that eliminate their dangling bonds. Their electronic structures and geometries are calculated and optimized (in static electric fields) *ab initio* in the singlet states.<sup>13</sup>

In Fig. 1 (down), we show several extended molecular orbitals (MOs) with a significant Ni-atomic orbital composition and a large probability density formed above the surface of the neutral nanocone in the *absence* of electric field. These MOs are less spread on the cone than the highest occupied molecular orbital (HOMO), shown last, and are shifted  $\approx 6$  eV above it, in the unbound part of the spectrum. In order to facilitate their population by one-photon processes, we can shift them closer to the HOMO by electric fields  $\mathcal{E}$  in the Stark effect.<sup>16</sup>

In the linear Stark effect,<sup>16</sup> the energy of a state  $|\Psi\rangle$  with no parity shifts in the static electric field  $\mathcal{E}$  by  $\Delta E = -\mathcal{E}\langle\Psi|d|\Psi\rangle$ , where  $d = er$  is the dipole operator. Other states might be shifted by the quadratic Stark effect.<sup>16</sup> Note that although carbon-capped SWCNTs are, in principle, stable at fields  $\mathcal{E} < 20$  V/nm,<sup>17</sup> their states are in fact metastable and can significantly emit electrons by tunneling at fields  $\mathcal{E} > 3-5$  V/nm.<sup>18</sup>

In Fig. 2, we present the electronic spectrum around the HOMO in the Ni-doped nanocone from Fig. 1, calculated in *static* electric fields,  $0 < \mathcal{E} < 20$  V/nm, oriented up along its ( $z$ ) axis. While the absolute shift of all the MOs depends on the position of the center of mass of the structure used in *ab initio* calculations ( $e\varphi$  term), the relative positions of the MOs are invariant on the center position. We can see that some virtual orbitals shift faster and form avoided crossing regions with other MOs on their way. The slowly shifting MOs are mostly composed of atomic orbitals of the aromatic carbon atoms. If electric field is applied parallel to the plane of benzene, the fastest fall in energies goes at a rate of  $0.4$  eV/V nm<sup>-1</sup>,<sup>19</sup> which is close to  $0.3$  eV/V nm<sup>-1</sup>, valid for these MOs in Fig. 2.

The fast shifting MOs in Fig. 2 are mostly composed of the extended Ni orbitals with large dipole matrix elements, shown in Fig. 1. They shift by the nonlinear Stark effect that

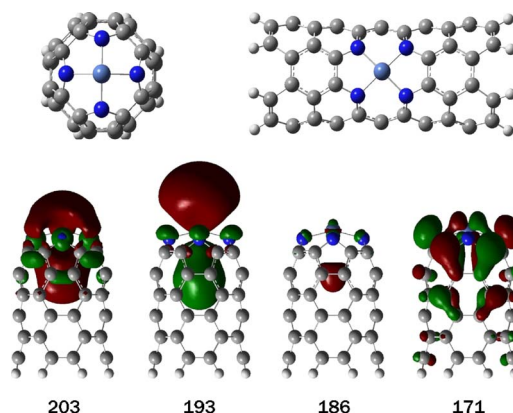


FIG. 1. (Color online) (Up left) Top view of the Ni-doped cone and (up right) (4,4) CNT. (Down) Extended MOs of the Ni-doped cone with a large metallic content. (Left to right) The MOs with large composition of the Ni orbitals: 7% 4s, 62% 5s, and 6% 6s ( $E_{203}=2.64$  eV); 2% 4s, 1% 5s, 12% 6s, and 50%  $11p_z$  ( $E_{193}=1.06$  eV); and 8% 5s and 84% 6s ( $E_{186}=0.24$  eV). (Last) The HOMO is spread more on the cone and substantially less away from it ( $E_{171}=-5.55$  eV).

<sup>a)</sup>Electronic mail: pkral@uic.edu

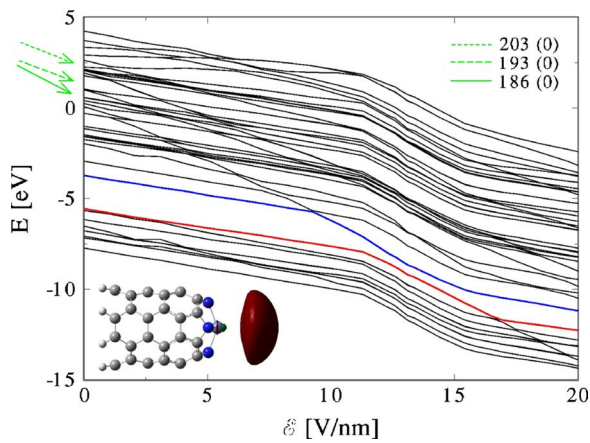


FIG. 2. (Color online) Dependence of the neutral Ni-doped nanocone MO energies on the strength of the electric field  $\mathcal{E}$ . The HOMO and the LUMO are shown by thick lines. The fast shifting 186th, 193th, and 203th MOs (at  $\mathcal{E}=0$  V/nm) are identified by arrows. The 186th MO that drops the fastest changes its Ni composition from 8%  $5s$  and 84%  $6s$  ( $\mathcal{E}=0$  V/nm) to 3%  $4s$ , 36%  $5s$ , and 49%  $6s$  ( $\mathcal{E}=10.3$  V/nm, LUMO) and 4%  $4s$ , 35%  $5s$ , and 47%  $6s$  ( $\mathcal{E}=15.4$  V/nm, HOMO). (Inset) The HOMO at electric field of 15.4 V/nm that contains mostly Ni  $s$  orbital contributions.

dominates at higher fields. The zero-field 186th MO with  $5-6s$  composition, depicted in Fig. 1, shifts the fastest at a rate of  $E \approx 0.7$  eV/V nm $^{-1}$ . This is close to that of the  $4s$  Li orbital in such fields, equal to  $E \approx 1.1$  eV/V nm $^{-1}$ .<sup>20</sup> At fields  $\mathcal{E} \approx 9$  V/nm, this MO forms a short avoided crossing with the lowest unoccupied molecular orbital (LUMO). As it approaches the HOMO, the HOMO-LUMO gap shrinks and an avoided crossing with the HOMO is formed in the wide region of the fields  $\mathcal{E} \approx 11-15$  V/nm. Here the two states become hybridized and the extended state gets populated, which is associated with a large variation of the electronic structure, due to different Coulombic couplings. At fields  $\mathcal{E} > 15$  V/nm, this MO continues shifting below the HOMO. Analogous electric-field-induced effects were also observed in BN nanotubes<sup>21</sup> and semiconductor nanocrystals.<sup>22</sup>

In Fig. 3 (up left to right), we demonstrate the total elec-

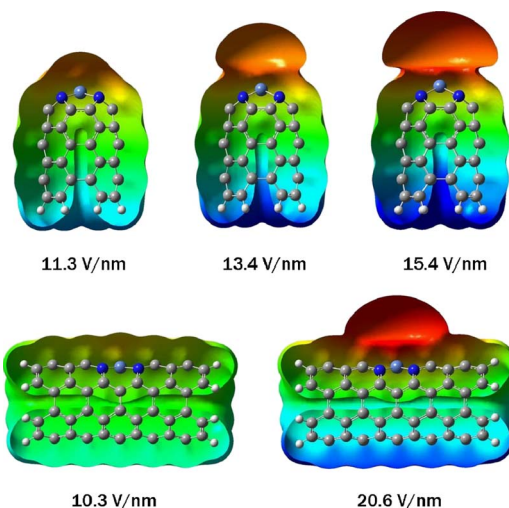


FIG. 3. (Color online) (Up, left to right) Extraction of the electron density from the Ni-doped nanocone in the static electric fields  $\mathcal{E}=11.3, 13.4,$  and  $15.4$  V/nm. (Down) Extraction of the electron density from the Ni-doped (4,4) CNT in  $\mathcal{E}=10.3$  (left) and  $20.6$  V/nm (right). In all the structures, the electrostatic potential in the interval  $\varphi=(-5.4, +5.4)$  V is mapped on the surface of the constant electron density of  $0.0004$  e/bohr $^3$ .

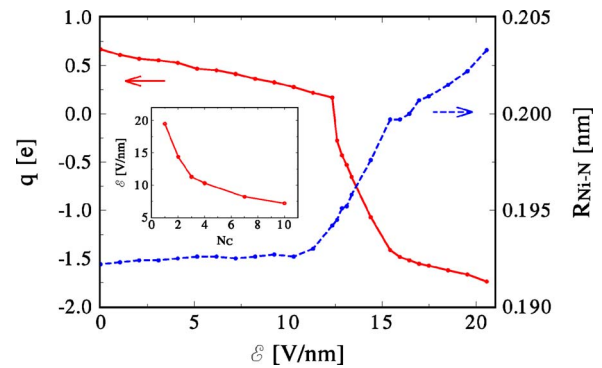


FIG. 4. (Color online) Dependence of the Ni atom Mulliken charge and the average Ni-N distance on the strength of the electric field for the Ni-doped nanocone. At the fields of  $\mathcal{E}=12.5-15$  V/nm, filling of the extended MO with the Ni character takes part, as the shifting MO hybridizes and forms avoided crossing first with the LUMO and then with the HOMO. This process is evidenced by the abrupt charging of Ni and prolongation of its bonds with the N atoms. (Inset) Dependence of the electric field needed for the filling of the extended states on the length of the nanocone (number of CNT's elementary cells).

tron density in the neutral Ni-doped nanocone for the electric fields  $\mathcal{E}=11.3, 13.4,$  and  $15.4$  V/nm, respectively. One can see the extraction of charge and formation of an extended “electron bag” above the cone, formed by the populated extended MOs. In Fig. 3 (down), we show the same in the metal-doped wall of the (4,4) SWCNT from Fig. 1, for the fields  $\mathcal{E}=10.3$  and  $20.6$  V/nm, oriented orthogonal to the plane with the four Ni atoms. Although these results were obtained in static fields, practical filling of these states can be only realized dynamically, due to their short field-emission lifetimes. We could use transport techniques<sup>23</sup> to describe their electrical and optical field-induced filling.

Coulombic coupling between the extended (populated) and other MOs leads to electronic and spatial restructurizations of the system. As we illustrate in Fig. 4, in the field  $0 < \mathcal{E} < 12.5$  V/nm, the positive Ni-atom charge gradually decreases, due to extraction of the cone electrons to its tip, whereas the average Ni-N bond length increases. In the fields  $\mathcal{E} \approx 12.5-15$  V/nm, the extended states are hybridized first with LUMO and then with HOMO, when they become filled by electrons. This is seen in the abrupt negative charging (electron population) of the Ni atom, accompanied by the HOMO gaining the Ni character, and by the resulting abrupt prolongation of the Ni-N bonds. At  $\mathcal{E} \approx 12.5$  and  $15$  V/nm, we can see breaks both in Figs. 2 and 4, signaling the beginning and the end of the filling process. Above  $\mathcal{E} \approx 15$  V/nm, the Ni states continue to move down and the HOMO is formed by other states. Finally, above  $\mathcal{E}=20$  V/nm, the Ni-N bond cleaves.

In the inset of Fig. 4, we show the dependence of the “minimum field” necessary for the electron extraction on the number of the carbon nanotube's elementary cells,  $N_C$ , in the nanocone [ $N_C=2$  in the structure from Fig. 3 (up)]. The field is substantially decreased for longer cones, since their polarization is larger, so that they could provide more electrons to the tip of the cones. In this way, one could populate the extended MOs even before the field gets too large, and the field-induced electron emission becomes significant, especially if this process is combined with their photoexcitation.

The electric field needed for filling of the extended MOs also depends strongly on the charge of the cone. For the cone in Fig. 3 with the charges of  $+2e, +1e, -1e,$  and  $-2e$  the

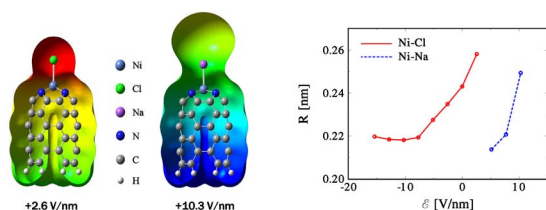


FIG. 5. (Color online) (Left) Binding to the neutral cone of the  $\text{Cl}^-$  anion, at  $\mathcal{E} \approx +2.6$  V/nm, and the  $\text{Na}^+$  cation, at  $\mathcal{E} = +10.3$  V/nm, close to their release fields from the structure. (Right) The Ni–Cl and Ni–Na distances plotted as a function of the field strength.

extraction fields are 18.2, 13.8, 7.5, and 6.5 V/nm, respectively (structures with odd number of electrons are calculated in triplet states). The decrease of the extraction field as the number of electrons increases is due to the shift of the HOMO up, leading to the formation of an avoided crossing with the shifting extended states at lower fields. On the other hand, filling of positively charged cones is harder also because electrons need to come from low energy MOs that are stronger bound to the positive nuclei. These results agree with the decrease of the extraction field for longer cones, shown in the inset of Fig. 4, where more electrons are effectively available at the cone tips at weaker fields, as the cone length is increased.

In fields of several V/nm, these extended MOs could have field-emission lifetimes of tens of femtoseconds, in analogy to other 4–6s atomic orbitals.<sup>20</sup> On the other hand, CNTs in the field of  $\mathcal{E} = 3$  V/nm have field-emission currents of  $j \approx 1$  nA,<sup>18</sup> i.e., one electron leaves every  $\approx 160$  ps. This slow electron emission very likely occurs from a localized state<sup>24</sup> or adsorbate on the CNTs<sup>25,26</sup> that are slowly repopulated after each event. Since filling of the extended states in metal-doped nanocones might be more easily controllable, they could be used in tunable electron emitters.<sup>17,25</sup>

The metal-doped nanocones might also be used to manipulate chemical bonds, ions, atoms, or molecules, in analogy to scanning tunneling microscopy (STM),<sup>27</sup> atomic force microscopy (AFM),<sup>28</sup> and other techniques.<sup>29</sup> External electric fields could control their binding and releasing with a higher precision than the STM and AFM systems. To follow this idea, we investigate binding of  $\text{Cl}^-$  and  $\text{Na}^+$  ions to the cone tip. In Fig. 5 (right), we show that the  $\text{Cl}^-$  anion that is added to the neutral cone system and placed at an expected binding distance from the metal binds to the positively charged Ni in the field range of  $-15.4 < \mathcal{E} < +2.6$  V/nm, where the Ni–Cl bond length is varied (the charged structure is calculated in the singlet state). The  $\text{Cl}^-$  anion detaches from the cone tip at  $\mathcal{E} \approx +2.6$  V/nm, when more electrons from the cone come to its tip and release the anion. We also test if the  $\text{Na}^+$  cation could bind to the positively charged Ni and find that in the field  $\mathcal{E} < +5$  V/nm there are not enough electrons. In the field range of  $+5.1 < \mathcal{E} < +10.3$  V/nm, more electrons from the structure come to the tip and provide weak binding of the  $\text{Na}^+$  cation. In Fig. 5 (left), we show that at the field  $\mathcal{E} = +10$  V/nm the electrons become highly extracted above the cone, partly due to the  $\text{Na}^+$  cation. They eventually populate the available Na states and release it.

We have introduced extended electronic states that are formed above metal-doped carbon nanostructures. The extended states could be used in electron emitters. These hybrid nanostructures could also bind ions, atoms, and molecular

ligands and be used in catalysis, molecular electronics, and various nanodevices.

This work was done with the use of the IBM P690 at the National Computational Science Alliance.

- <sup>1</sup>T. Gallagher, *Rydberg Atoms* (Cambridge University Press, New York, 1994).
- <sup>2</sup>C. H. Greene, A. S. Dickinson, and H. R. Sadeghpour, Phys. Rev. Lett. **85**, 2458 (2000).
- <sup>3</sup>B. E. Granger, P. Král, H. R. Sadeghpour, and M. Shapiro, Phys. Rev. Lett. **89**, 135506 (2002).
- <sup>4</sup>D. Segal, B. E. Granger, H. R. Sadeghpour, P. Král, and M. Shapiro, Phys. Rev. Lett. **94**, 016402 (2005).
- <sup>5</sup>M. Zamkov, N. Woody, S. Bing, H. S. Chakraborty, Z. Chang, U. Thumm, and P. Richard, Phys. Rev. Lett. **93**, 156803 (2004).
- <sup>6</sup>S. R. Stoyanov and P. Král, J. Phys. Chem. B **110**, 21480 (2006).
- <sup>7</sup>K. M. Kadish, K. M. Smith, and R. Guilard, *The Porphyrine Handbook* (Academic, San Diego, 1999).
- <sup>8</sup>S. Ma and H.-C. Zhou, J. Am. Chem. Soc. **128**, 11734 (2006).
- <sup>9</sup>A. Tsuda and A. Osuka, Science **293**, 79 (2001); R. Harada and T. Kojima, Chem. Commun. (Cambridge) **2005**, 716.
- <sup>10</sup>I. Barth and J. Manz, Arch. Eisenhuettenwes. **45**, 2962 (2006).
- <sup>11</sup>D. S. Hecht, R. A. Ramirez, E. Artukovic, M. Briman, K. Chichak, J. F. Stoddart, and G. Grüner, Nano Lett. **9**, 2031 (2006).
- <sup>12</sup>M. Terrones, P. M. Ajayan, F. Banhart, X. Blase, D. L. Carroll, J. C. Charlier, R. Czerw, B. Foley, N. Grobert, R. Kamalakaran, P. Rohler-Redlich, M. Rühle, T. Seeger, and H. Terrones, Appl. Phys. A: Mater. Sci. Process. **74**, 355 (2002).
- <sup>13</sup>We use the B3LYP exchange-correlation functional, incorporated in the GAUSSIAN03 software package (Ref. 14). For the Ni atom, we use the Stuttgart-Dresden (SDD) effective core potential for the core electrons and the SDD basis set for the valence electrons (Ref. 15). For all other atoms, we use the all-electron split-valence 3–21G\* basis set.
- <sup>14</sup>M. J. Frisch, G. W. Trucks, H. B. Schlegel, G. E. Scuseria, M. A. Robb, J. R. Cheeseman, J. A. Montgomery, Jr., T. Vreven, K. N. Kudin, J. C. Burant, J. M. Millam, S. S. Iyengar, J. Tomasi, V. Barone, B. Mennucci, M. Cossi, G. Scalmani, N. Rega, G. A. Petersson, H. Nakatsuji, M. Hada, M. Ehara, K. Toyota, R. Fukuda, J. Hasegawa, M. Ishida, T. Nakajima, Y. Honda, O. Kitao, H. Nakai, M. Klene, X. Li, J. E. Knox, H. P. Hratchian, J. B. Cross, V. Bakken, C. Adamo, J. Jaramillo, R. Gomperts, R. E. Stratmann, O. Yazyev, A. J. Austin, R. Cammi, C. Pomelli, J. W. Ochterski, P. Y. Ayala, K. Morokuma, G. A. Voth, P. Salvador, J. J. Dannenberg, V. G. Zakrzewski, S. Dapprich, A. D. Daniels, M. C. Strain, O. Farkas, D. K. Malick, A. D. Rabuck, K. Raghavachari, J. B. Foresman, J. V. Ortiz, Q. Cui, A. G. Baboul, S. Clifford, J. Cioslowski, B. B. Stefanov, G. Liu, A. Liashenko, P. Piskorz, I. Komaromi, R. L. Martin, D. J. Fox, T. Keith, M. A. Al-Laham, C. Y. Peng, A. Nanayakkara, M. Challacombe, P. M. W. Gill, B. Johnson, W. Chen, M. W. Wong, C. Gonzalez, and J. A. Pople, GAUSSIAN 03, Revision D.01, Gaussian, Inc., Wallingford, CT, 2004.
- <sup>15</sup>M. Dolg, U. Wedig, H. Stoll, and H. Preuss, J. Chem. Phys. **86**, 2123 (1987); D. Andrae, U. Hauessermann, M. Dolg, H. Stoll, and H. Preuss, Theor. Chim. Acta **77**, 123 (1990).
- <sup>16</sup>A. S. Davidov, *Quantum Mechanics* (Pergamon, Oxford, 1965).
- <sup>17</sup>C. Kim, B. Kim, S. Lee, C. Jo, and Y. Lee, Appl. Phys. Lett. **79**, 1187 (2001); Phys. Rev. B **65**, 165418 (2002).
- <sup>18</sup>J.-M. Bonard, K. A. Dean, B. F. Colle, and C. Klinck, Phys. Rev. Lett. **89**, 197602 (2002).
- <sup>19</sup>Y. C. Choi, W. Y. Kim, K.-S. Park, P. Tarakeshwar, K. S. Kim, T.-S. Kim, and J. Y. Lee, J. Chem. Phys. **122**, 094706 (2005).
- <sup>20</sup>S. I. Themelis and C. A. Nicolaides, J. Phys. B **34**, 2905 (2001).
- <sup>21</sup>M. Ishigami, J. D. Sau, S. Aloni, M. L. Cohen, and A. Zettl, Phys. Rev. Lett. **94**, 056804 (2005).
- <sup>22</sup>K. Becker, J. Lupton, J. Muller, A. L. Rogach, D. V. Talapin, H. Weller, and J. Feldmann, Nat. Mater. **5**, 777 (2006).
- <sup>23</sup>P. Král and A. P. Jauho, Phys. Rev. B **59**, 7656 (1999).
- <sup>24</sup>T. Kuzumaki, Y. Takamura, H. Ichinose, and Y. Horiike, Appl. Phys. Lett. **78**, 3699 (2001).
- <sup>25</sup>K. A. Dean and B. R. Chalamala, Appl. Phys. Lett. **76**, 375 (2000).
- <sup>26</sup>J. Cumings, A. Zettl, M. R. McCartney, and J. C. H. Spence, Phys. Rev. Lett. **88**, 056804 (2002).
- <sup>27</sup>G. Binnig and H. Rohrer, IBM J. Res. Dev. **30**, 355 (1986).
- <sup>28</sup>A.-S. Duwez, S. Cuenot, C. Jérôme, S. Gabriel, R. Jérôme, S. Rapino, and F. Zerbetto, Nature Nanotechnology **1**, 122 (2006).
- <sup>29</sup>B. Wang and P. Král, J. Am. Chem. Soc. **128**, 15984 (2006).